

Current control in soft-wall focusing electron billiards: energy-persistent scattering in the deep quantum regime

C. Morfonios¹ and P. Schmelcher^{1,2}

¹*Zentrum für Optische Quantentechnologien, Universität Hamburg, Luruper Chaussee 149, 22761 Hamburg, Germany*

²*The Hamburg Centre for Ultrafast Imaging, Universität Hamburg, Luruper Chaussee 149, 22761 Hamburg, Germany*

(Dated: February 21, 2014)

The isolation of energetically persistent scattering pathways from the resonant manifold of an open electron billiard in the deep quantum regime is demonstrated. This enables efficient conductance switching at varying temperature and Fermi velocity, using a weak magnetic field. The effect relies on the interplay between magnetic focusing and soft-wall confinement, which rescale the scattering pathways and decouple quasi-bound states from the attached leads. The mechanism proves robust against billiard shape variations and qualifies as a nanoelectronic current control element.

PACS numbers: 73.23.Ad, 85.35.Ds, 73.63.Kv, 75.47.-m

The control of charge flow in low-dimensional quantum systems lies at the heart of nanoelectronic circuit design, posing the challenge to understand and manipulate the mechanisms that enable its realization. Prominent candidate elements for conductance control are open electron billiards [1–6], which can be patterned to almost arbitrary shapes well below the electronic mean free path and coherence length [7–9], and whose transport properties are drastically altered by an externally applied magnetic field [10–17]. They therefore dominate the intense investigation of coherent magnetotransport in the mesoscopic regime, where quantum interference phenomena meet and overlap with the notion of oriented particle paths. Specifically, generalized Aharonov-Bohm (AB) oscillations [18] from phase modulation of interfering states [11, 15, 19] combine with the Lorentz deflection [20, 21] of electrons up to the formation of edge states [11, 16, 22]. An intriguing question is how to separate these two types of magnetotransport dynamics, phase- versus path-dominated, in a regime where they strongly overlap. This would correspond to the suppression of quantum fluctuations in favor of directed pathways, at wavelengths comparable to the system size. From an experimental viewpoint, the magnetic field provides a unique macroscopic handle on those mesoscopic processes determining the conductance of the system, and the challenge is to find a way to control them under ‘comfortable’ conditions. In other words: How can a weak magnetic field switch the current flow through a sizable electron billiard at low bias and finite temperature, and over a broad Fermi level variation? The answer lies in identifying and designing transport mechanisms which respond reliably to changes in the field strength while remaining robust against variations in energy, and at the same time stay separated from omnipresent quantum fluctuations. The key feature in the observable response consists in a controllable background transmission, magnetically switched between its extrema, upon which only narrow interference-induced Fano resonances [23] are superimposed [3, 5, 24]. This requires energetically persistent scattering pathways that mediate transport or cause complete reflection, but interfere only weakly with resonant states.

In the present work, we realize the above scenario in an open electron billiard with an elliptical ‘soft wall’ po-

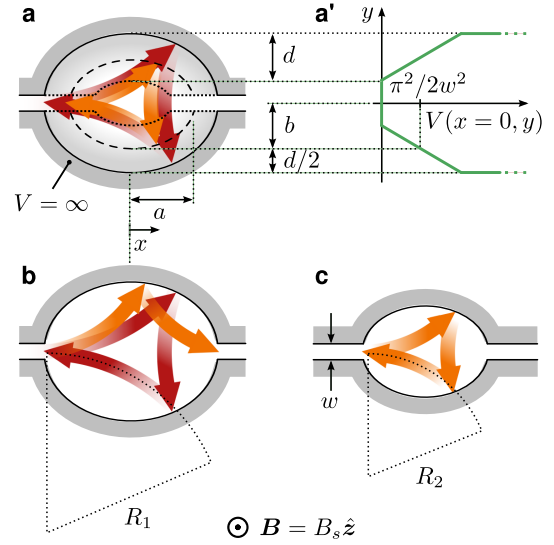


FIG. 1. (Color online) System setup and sketch of magnetically focused pathways. (a) Electron billiard defined by hard-wall confinement (solid line) and a soft-wall potential $V(x, y)$ decreasing along elliptical contours to zero (dotted contour), with wall width d in the x - and y -directions. The wall opens up along $y = 0$ to attached leads of width w , and its central contour (dashed) has semi-axes a and b . (a') Cross section at $x = 0$ for linear wall potential, with central contour lying at the threshold of the first propagating channel. (b) Without the soft wall, a magnetically focused, backscattered pathway (with cyclotron radius R_1 , red arrows) eventually turns into a transmitted pathway (with cyclotron radius $R_2 < R_1$, orange arrows) for sufficient decrease in energy, while (c) backscattering would be retained for a correspondingly smaller billiard. With appropriately chosen potential in (a), similar backscattered paths can persist with varying energy for a common field strength B_s . The arrows sketch the overall electronic motion.

tential (see Fig.1). The experimental setup in mind is a quantum dot with steep boundary potential [8, 9] supplied with additional peripheral gates [7] which further deplete the internal 2D electronic motion. With a perpendicular magnetic field \mathbf{B} piercing the dot, the combination of the elongated lateral shape with the soft wall enables an energy-invariant switching mechanism by isolating the required scattering pathways from the manifold of resonant levels. In short: For $B = 0$, the elliptic soft

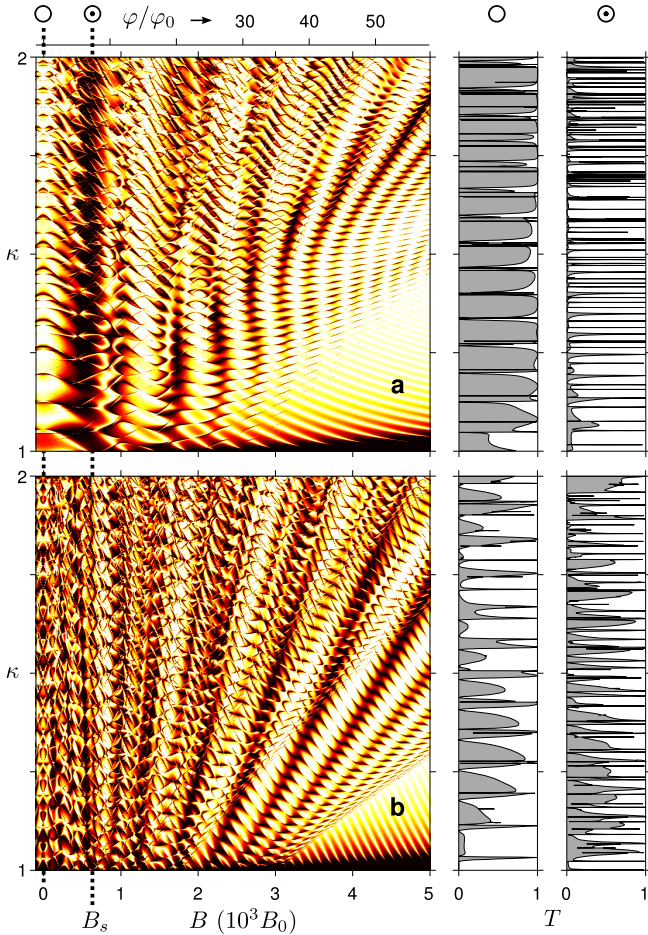


FIG. 2. (Color online) Transmission (from 0-black to 1-white) as a function of magnetic field strength B (or flux quanta φ) and scaled incoming momentum $\kappa = p_{\text{in}}w/\pi$ within the first open channel $1 < \kappa < 2$ of the attached leads, for (a) a billiard with the soft-wall potential of Fig. 1(a') with $(a, b, d, w) = (84, 128, 96, 32) a_0$, and (b) the same billiard without soft wall. Right panels: cuts through the $T(B, \kappa)$ -maps at zero field (marked \odot) and at the switching field $B_s = 0.63 \times 10^{-3} B_0$ (marked \odot) or flux $\varphi_s = 7.32 \varphi_0$ (where $\varphi_0 = h/e = \pi$ is the flux quantum). For a reference length unit $a_0 = 2$ nm, the field strength unit is $B_0 = \hbar/ea_0^2 = 164.55$ T.

walls collimate the electronic motion into the longitudinal direction, causing high overall transmission. At a special 'switching' field strength $B = B_s$, the incoming electrons are focused [22] into a completely backscattered pathway, which becomes geometrically rescaled in the presence of the soft wall (as sketched by the arrows in Fig. 1). In both cases, the crucial role of the soft wall is thus to create *energetically persistent* scattering pathways while decoupling localized resonant states from the openings. As a result, the setup enables efficient finite-temperature current switching for varying Fermi energy, by turning on a weak external magnetic field.

With decohering electrodes implemented by attached semi-infinite leads, the effective (energy dependent and non-Hermitian [25]) Hamiltonian of the open system is represented on a tight-binding lattice, and the transmission function T is computed via an extended recursive Green function scheme [16]. The conductance G at Fermi energy E_F and temperature Θ is then ob-

tained within the Landauer-Büttiker framework [25]. The choice $\hbar = e = m = a_0 \equiv 1$ fixes the units of energy $E_0 = \hbar^2/ma_0^2$ and magnetic field strength $B_0 = \hbar/ea_0^2$ for given effective mass m and lattice constant a_0 .

The transmission through the billiard with and without soft-wall is shown in Fig. 2 as a function of B and incoming momentum κ , which we will refer to as 'maps'. Qualitatively common features in the two $T(B, \kappa)$ -maps are: isolated edge state peaks [22] at high B and low κ (lower right corner) as well as stripe-like interference patterns from multiple populated edge states [11] for higher κ (lower diagonal half), which become less pronounced and eventually destroyed by generalized AB interference of spatially extended states [15, 19] at lower B (upper diagonal half). The slope of the characteristic reflection and transmission stripes in the maps portrays the formation of skipping [22] orbits within the billiard, whose cyclotron radius scales like $R \sim \sqrt{p_{\text{in}}^2 - 2V}/B$. Without the soft wall [Fig. 2(b)], the approximate commensurability between the skipping intervals and the (half) length of the boundary is preserved along lines of positive slope in the (B, κ) -plane on which high reflection (transmission) occurs. The soft wall causes the stripes to bend around the middle of the channel [Fig. 2(a)], which shows that the finite potential effectively reduces the size of the billiard area at low κ : A stronger focusing field is needed to maintain the high or low T for decreasing κ , and consequently the map features broaden along the B -axis.

In the present context, the extraordinary effect of the soft wall is manifest in the low- B regime, where the very complex dynamics generally induces highly irregular interference contributions: At a relatively weak field $B = B_s$, backscattering persists over the whole channel and completely dominates the background transmission spectrum, forming a broad and vertical reflection stripe in the $T(B, \kappa)$ -map, upon which only very narrow Fano resonances are superimposed (see Fig. 2(a)). Indeed, background transmission does not set in again until the second channel threshold. This remarkable feature, which is absent without the soft wall (see Fig. 2(b)), is reversed when the field is turned off: For $B = 0$, a highly transmitting background is only slightly perturbed by narrow resonant dips (see cuts through $T(B, \kappa)$ -maps in Fig. 2). At finite temperature, the dips (peaks) at $B = 0$ ($B = B_s$) are effectively washed away by the thermal contribution of the highly transmitting (reflecting) non-resonant states around the Fermi level. This is seen in Fig. 3(a,a'), where the conductance is kept close to unity (zero) over a broad range in E_F even at considerable thermal width $k_B\Theta$.

To understand the influence of the proposed type of soft wall potential, and the induced mechanism underlying conductance control, let us analyze the electronic scattering states responsible for high (low) background transmission in the absence (presence) of the field. Fig. 3(b,b') displays the local density of states (LDOS) $\rho(x, y; \kappa)$ for electrons incident in the left lead of the billiard at sample non-resonant energies.

For $B = 0$ (Fig. 3(b)), we see that the effect of the finite potential is to direct the motion along the axis connecting the leads, thus enhancing transmission. This is achieved in a twofold way: (i) The special shape of the potential around the lead openings, forming a stub of free motion

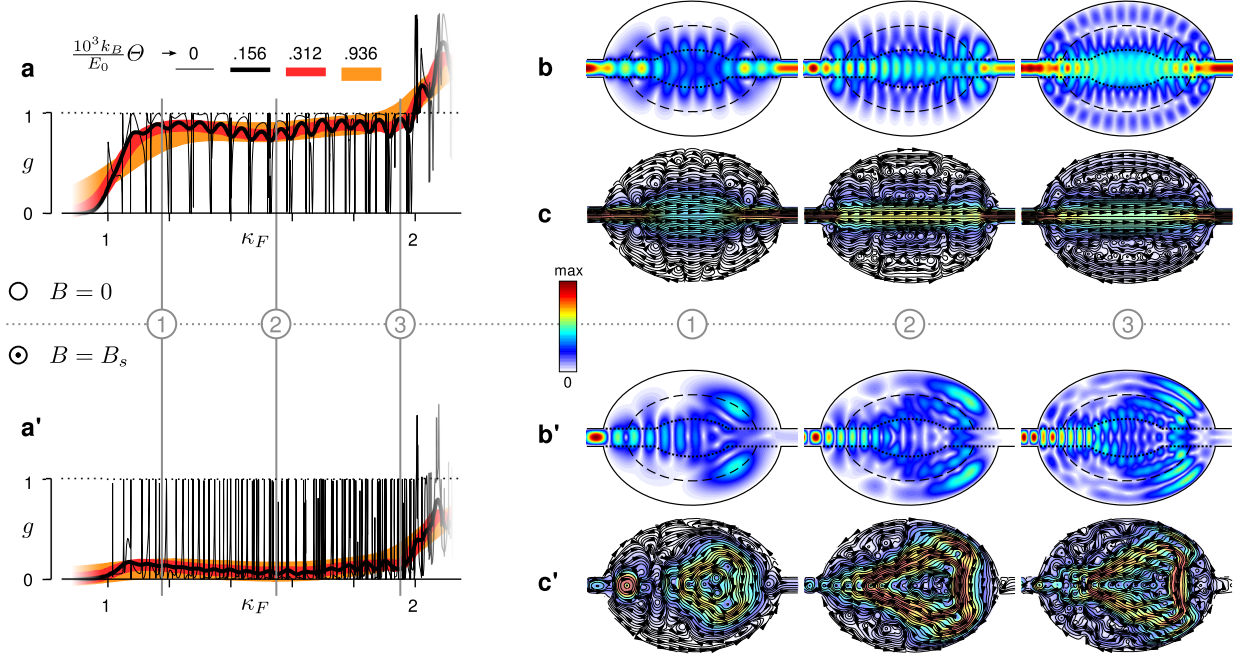


FIG. 3. (Color online) (a) Dimensionless conductance $g = G/G_0$ (with quantum $G_0 = 2e^2/h$) around the first open channel for $B = 0$, for the same billiard as in Fig. 2(a), at different temperatures Θ . With $a_0 = 2$ nm and $m = 0.069 m_e$ (transport at a GaAs/AlGaAs interface): $E_0 = 276$ meV and $\Theta = 0, 0.5, 1.0, 3.0$ K. (b) Scaled LDOS $\sqrt{\rho}$ and (c) scaled probability current density $\sqrt{|\mathbf{j}|}$ (the flow of \mathbf{j} is depicted by directed streamlines) shown at momenta $\kappa_{1,2,3}$ indicated by vertical lines in (a), for electrons incident in the left lead (colormap normalized to maximum value in each plot). The dashed (dotted) line in (b,b') shows the potential contour at $V = \pi^2/2w^2$ ($V = 0$). (a',b',c') Same as above, but for $B = B_s$.

into the billiard as a prolongation of each lead, suppresses the transversal component of the electronic local momentum, thereby collimating [22] the motion in forward direction (in other words, the soft wall reduces the diffractive effect of the hard-wall lead openings). (ii) Owing to its elliptic contour, the soft wall depletes the scattering state along the billiard boundary and further confines it into an elongated profile leaking into both leads. For the same reason, states corresponding to distinct Fano resonances become well decoupled from the leads, and thus isolated from a significant (subtractive) contribution to the overall transport.

For $B = B_s$ (Fig. 3(b')), the scattering state profiles reveal the key role of the soft wall in energetically sustaining the backscattered pathways. Again, the mechanism is twofold: (i) States strongly coupled to the incoming lead are now magnetically focused onto the billiard boundary, so that the electron follows a pathway which is backscattered after ‘bouncing’ twice off the boundary. The soft wall here crucially comes to the aid of conductance suppression by ‘rescaling’ the dynamics and thus keeping the non-resonant backscattered pathway energetically invariant: With increasing (decreasing) kinetic energy, the electron undergoes weaker (stronger) Lorentz deflection at constant $B = B_s$, but at the same time penetrates more (less) into the soft wall potential towards the boundary (compare outer lobes of ρ in Fig. 3(b';1,2,3)). The soft wall thus effectively increases the billiard size with energy, and as a result, the magnetically focused, backscattered pathway persists over the whole channel. (ii) As in the field-free case, any long-lived resonant states are further confined away from both leads by the soft wall, rendering

the corresponding Fano peaks extremely narrow.

The actual electronic motion in the billiard is depicted in Fig. 3(c,c')) through its probability current density $\mathbf{j}(x, y; \kappa)$. With or without magnetic field, the wave nature of transport leads to multiple complex vortex structures covering the billiard, which change dramatically in energy. Nevertheless, we see that the parts of the flow with higher density indeed favor motion along the above described pathways needed for conductance switching in varying E_F , that is, a forward collimated current for $B = 0$ and a circulating backscattered current for $B = B_s$.

It should be pointed out that, although the soft wall succeeds in geometrically ‘rescaling’ the low-field (two-bounce) backscattered pathway, the motion is in general drastically modified from that in a corresponding purely hard-wall billiard with spectral boundary reflection [17]. In the present case, the more it is magnetically deflected due to its reduced (local) momentum, and the motion is further affected by continuous electrostatic refraction [26]. These effects are enhanced at stronger fields which localize the scattering states closer to the boundary over longer parts (unlike the two-bounce paths, which predominantly enter the wall radially). Therefore, such higher order (four-bounce, six-bounce, etc.) backscattered pathways [12] cannot persist over large energy intervals for the same potential. Indeed, in Fig. 2(a) vertical reflection stripes tend to form also at higher field strengths ($B/B_0 \approx 1.8, 2.2$, etc.), but are eventually tilted or destroyed as energy varies. Switching efficiency is thus restricted to smaller κ_F -range and lower Θ at these fields.

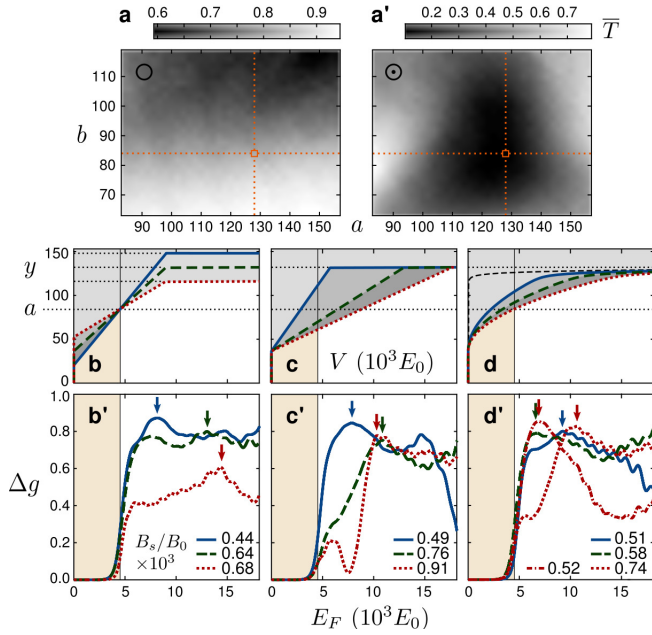


FIG. 4. (Color online) (a,a'): Mean transmission in the first channel, \bar{T} , for varying mid-wall semi-axes a and b of the billiard with linear wall potential in Fig. 1(a,a') with $d = 96 a_0$, at (a) $B = 0$ and (a') $B = B_s$. The dotted lines indicate the geometry $(a, b) = (128, 84) a_0$ chosen in Figs. 2, 3 and below. (b,c,d): Cross-section $V(x=0, y)$ for (b) varying wall width and (c) varying wall slope for a linear wall profile and (d) varying steepness for a parabolic soft wall profile with Wood-Saxon-type [28] boundary (thin dashed line). (b',c',d'): corresponding conductance change $\Delta g = g_{B=0} - g_{B=B_s}$ at $k_B\Theta/E_0 = 0.312 \times 10^{-3}$ for optimal switching field strengths B_s (shown in the legends), within the first open channel (channel threshold indicated by vertical lines). Both dotted and dash-dotted lines in (d') correspond to the dotted potential profile in (d), but for different B_s . Arrows indicate the maximum of each curve. Lengths are in units of a_0 . For $a_0 = 2$ nm and $m = 0.069 m_e$: $E_0 = 276$ meV and $\Theta = 1.0$ K.

Having demonstrated and explained the proposed mechanism for finite-temperature, energy-invariant conductance switching, we finally analyze the impact of setup variations. In Fig. 4(a,a'), the channel-averaged transmission $\bar{T} = \int_1^2 T(\kappa) d\kappa$, a simple estimate of the overall transmittivity, is shown for varying lateral shape of the billiard. The substantial overlap of zero-field high- \bar{T} and switching-field low- \bar{T} areas indicates the robustness of the switching effect against alteration of the dot shape. For a chosen shape, Fig. 4(b',c',d') shows the switching contrast $\Delta g = g_{B=0} - g_{B=B_s}$ at a reference broadening $k_B\Theta$ for different soft wall profiles, including ones (d) that simulate a concrete experimental setup [7–9]. Note that high switching efficiency relies on the suppressed $g_{B=B_s}$ of a single and relatively large billiard (of area $\pi(a + \frac{d}{2})(b + \frac{d}{2}) \gg w^2$, containing $\gtrsim 130$ levels at $B = 0$), and is achieved for a broad variety of soft wall profiles [27]. The optimal switching field B_s generally increases with the steepness of the wall potential, in accordance with the stronger confinement of low-energy backscattering billiard states. Further, the curves demonstrate that optimal switching (maximal Δg , see arrows in Fig. 4(b',c',d')) can be adjusted to different E_F by changing the soft wall parameters. For some setups (dot-

ted line in (d)), energy-persistent backscattering occurs for distinct B_s -values along separate parts of the channel, meaning that optimal E_F for switching can be magnetically tuned in this case (see dotted and dash-dotted lines in (d'), showing large Δg in the upper and lower channel half, respectively).

In conclusion, we have demonstrated a simple way to isolate magnetically focused, backscattered pathways from the manifold of resonant levels of a large electron billiard, and make these pathways persistent in energy. The underlying mechanism relies on the combined action of an elongated (elliptic) billiard boundary and a designed soft-wall potential, which together decouple quasi-bound states from the attached leads while geometrically rescaling the backscattered paths. With the field-free motion simultaneously collimated for high transmission, the proposed setup constitutes an efficient and robust conductance switching device at finite temperature and low field strength over broad Fermi level variation. Its experimental realization is feasible, e.g., in Ga[Al]As heterostructures by a combination of local oxidation techniques with optical or electron-beam lithography [7–9]. This provides a high precision in lateral dot shape with steep soft-wall potential corresponding to a depletion length $\gtrsim 15$ nm [8]. The quantum dot can be tuned by additional top or planar gates [7, 8], and large electron mean free paths are achievable at substantial thermal width. Example values for the latter are 3–5 μm at 4.2 K [9].

The authors are thankful to P. Giannakeas for valuable discussions.

-
- [1] I. V. Zozoulenko and K.-F. Berggren, Phys. Rev. B **56**, 6931 (1997).
 - [2] R. G. Nazmitdinov, K. N. Pichugin, I. Rotter, and P. Šeba, Phys. Rev. B **66**, 085322 (2002).
 - [3] B. Weingartner, S. Rotter, and J. Burgdörfer, Phys. Rev. B **72**, 115342 (2005).
 - [4] A. F. Sadreev, E. N. Bulgakov and I. Rotter, Phys. Rev. B **73**, 235342 (2006).
 - [5] E. R. Racec, U. Wulf, and P. N. Racec, Phys. Rev. B **82**, 085313 (2010).
 - [6] S. Rotter, P. Ambichl, and F. Libisch, Phys. Rev. Lett. **106**, 120602 (2011).
 - [7] A. Fuhrer, S. Lüscher, T. Heinzel, K. Ensslin, W. Wegscheider, and M. Bichler, Phys. Rev. B **63**, 125309 (2001).
 - [8] T. Heinzel, R. Held, S. Lüscher, K. Ensslin, W. Wegscheider, and M. Bichler, Physica E **9**, 84 (2001).
 - [9] V. I. Borisov, V. G. Lapin, V. E. Sizov, and A. G. Temiryazev, Zhur. Tekh. Fiz. **37**, 85 (2011) [Tech. Phys. Lett. **37**, 136 (2011)].
 - [10] I. V. Zozoulenko, A. S. Sachrajda, C. Gould, K.-F. Berggren, P. Zawadzki, Y. Feng and Z. Wasilewski, Phys. Rev. Lett. **83**, 1838 (1999).
 - [11] S. Rotter, B. Weingartner, N. Rohringer, and J. Burgdörfer, Phys. Rev. B **68**, 165302 (2003).
 - [12] R. Brunner, R. Meisels, F. Kuchar, R. Akis, D. K. Ferry, and J. P. Bird, Phys. Rev. Lett. **98**, 204101 (2007).
 - [13] D. Buchholz, P. Drouvelis, and P. Schmelcher, Europhys. Lett. **81**, 37001 (2008).
 - [14] C. Payette, G. Yu, J. A. Gupta, D. G. Austing, S. V. Nair, B. Partoens, S. Amaha, and S. Tarucha, Phys. Rev. Lett. **102**, 026808 (2009).

- [15] C. Morfonios, D. Buchholz, and P. Schmelcher, Phys. Rev. B **80**, 035301 (2009).
- [16] C. Morfonios, D. Buchholz, and P. Schmelcher, Phys. Rev. B **83**, 205316 (2011).
- [17] N. Aoki, R. Brunner, A. M. Burke, R. Akis, R. Meisels, D. K. Ferry, and Y. Ochiai, Phys. Rev. Lett. **108**, 136804 (2012).
- [18] Y. Aharonov and D. Bohm, Phys. Rev. **115**, 485 (1959).
- [19] U. Sivan, Y. Imry, and C. Hartzstein, Phys. Rev. B **39**, 1242 (1989).
- [20] B. Szafran and F. M. Peeters, Europhys. Lett. **70**, 810 (2005).
- [21] M. R. Poniedzialek and B. Szafran, J. Phys.: Condens. Matter **24**, 085801 (2012).
- [22] C. W. J. Beenakker and H. van Houten, in *Solid State Physics*, edited by H. Ehrenreich and D. Turnbull (Academic, New York, 1991), Vol. 44, p. 1.
- [23] U. Fano, Phys. Rev. **124**, 1866 (1961).
- [24] A. E. Miroshnichenko, S. Flach, and Y. S. Kivshar, Rev. Mod. Phys. **82**, 2257 (2010).
- [25] S. Datta, *Electronic Transport in Mesoscopic Systems* (Cambridge University Press, Cambridge, UK, 1995).
- [26] J. Repp, G. Meyer and K.-H. Rieder, Phys. Rev. Lett. **92**, 036803 (2004).
- [27] In Ref. [12], a magnetoresistance resonance is caused by cascading of similar backscattered states in an array of smaller billiards (relative to lead openings) at 10 mK.
- [28] F. J. Betancur, I. D. Mikhailov, and L. E. Oliveira, J. Phys. D: Appl. Phys. **31** 3391 (1998).